10320 Camino Santa Fe, Suite G
San Diego, CA 92121
Tel: 858.875.1900 Fax: 858.875.1999

GAPDH Antibody
Purified Mouse Monoclonal Antibody (Mab)
Catalog # AM1020b

Specification

GAPDH Antibody - Product Information

Application	**WB, IF, IHC-P,E**
Primary Accession	P04406
Reactivity	**Human, Mouse, Rat**
Host	**Mouse**
Clonality	**Monoclonal**
Isotype	**IgG1**

GAPDH Antibody - Additional Information

Gene ID 2597

Other Names
Glyceraldehyde-3-phosphate dehydrogenase, GAPDH, Peptidyl-cysteine S-nitrosylase GAPDH, 2699-, GAPDH, GAPD

Target/Specificity
GAPDH recombinant protein is used to produce this monoclonal antibody.

Dilution
WB~~1:2000~10000
IF~~1:25
IHC-P~~1:25

Format
Purified monoclonal antibody supplied in PBS with 0.09% (W/V) sodium azide. This antibody is purified through a protein G column, followed by dialysis against PBS.

Storage
Maintain refrigerated at 2-8°C for up to 2 weeks. For long term storage store at -20°C in small aliquots to prevent freeze-thaw cycles.

Precautions
GAPDH Antibody is for research use only and not for use in diagnostic or therapeutic procedures.

GAPDH Antibody - Protein Information

Name GAPDH {ECO:0000303|PubMed:2987855, ECO:0000312|HGNC:HGNC:4141}

Function Has both glyceraldehyde-3-phosphate dehydrogenase and nitrosylase activities, thereby playing a role in glycolysis and nuclear functions, respectively (PubMed:11724794, PubMed:3170585). Glyceraldehyde-3-phosphate dehydrogenase is a key enzyme in glycolysis that catalyzes the first step of the pathway by converting D- glyceraldehyde 3-phosphate (G3P) into

3-phospho-D-glyceroyl phosphate (PubMed:11724794, PubMed:3170585). Modulates the organization and assembly of the cytoskeleton (By similarity). Facilitates the CHP1- dependent microtubule and membrane associations through its ability to stimulate the binding of CHP1 to microtubules (By similarity). Component of the GAIT (gamma interferon-activated inhibitor of translation) complex which mediates interferon-gamma-induced transcript-selective translation inhibition in inflammation processes (PubMed:23071094). Upon interferon-gamma treatment assembles into the GAIT complex which binds to stem loop-containing GAIT elements in the 3'-UTR of diverse inflammatory mRNAs (such as ceruplasmin) and suppresses their translation (PubMed:23071094). Also plays a role in innate immunity by promoting TNF-induced NF-kappa-B activation and type I interferon production, via interaction with TRAF2 and TRAF3, respectively (PubMed:23332158, PubMed:27387501). Participates in nuclear events including transcription, RNA transport, DNA replication and apoptosis (By similarity). Nuclear functions are probably due to the nitrosylase activity that mediates cysteine S-nitrosylation of nuclear target proteins such as SIRT1, HDAC2 and PRKDC (By similarity).

Cellular Location
Cytoplasm, cytosol. Nucleus {ECO:0000250|UniProtKB:P04797}. Cytoplasm, perinuclear region. Membrane Cytoplasm, cytoskeleton {ECO:0000250|UniProtKB:P04797} Note=Translocates to the nucleus following S-nitrosylation and interaction with SIAH1, which contains a nuclear localization signal (By similarity). Postnuclear and Perinuclear regions (PubMed:12829261) {ECO:0000250|UniProtKB:P04797, ECO:0000269|PubMed:12829261}

GAPDH Antibody - Protocols

Provided below are standard protocols that you may find useful for product applications.

- Western Blot
- Blocking Peptides
- Dot Blot
- Immunohistochemistry
- Immunofluorescence
- Immunoprecipitation
- Flow Cytomety
- Cell Culture

GAPDH Antibody - Images

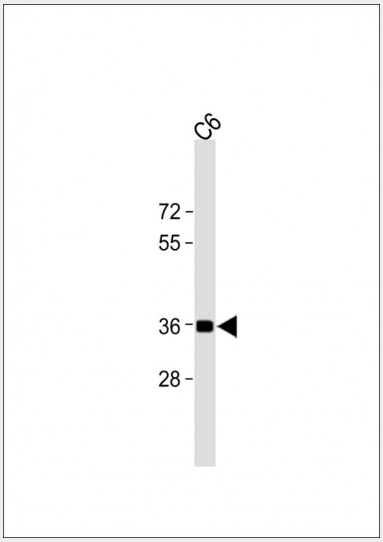

10320 Camino Santa Fe, Suite G
San Diego, CA 92121
Tel: 858.875.1900 Fax: 858.875.1999

All lanes: Anti-GAPDH Antibody at 1:1000 dilution + C6 whole cell lysate Lysates/proteins at 20 µg per lane. Secondary Goat Anti-mouse IgG, (H+L), Peroxidase conjugated (ASP1613) at 1/15000 dilution. Observed band size: 36KDa Blocking/Dilution buffer: 5% NFDM/TBST.

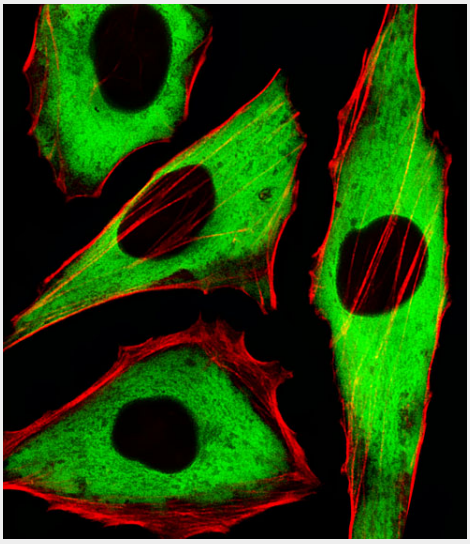

Fluorescent image of Hela cells stained with XAF1 GAPDH Antibody(Cat#AM1020b). AM1020b was diluted at 1:25 dilution. An Alexa Fluor® 488-conjugated goat anti-mouse lgG at 1:400 dilution was used as the secondary antibody (green). Cytoplasmic actin was counterstained with Alexa Fluor® 555 conjugated with Phalloidin (red).

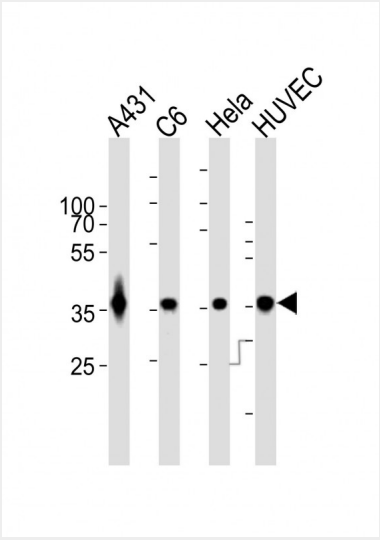

All lanes : Anti-GAPDH Antibody at 1:1000 dilution Lane 1: A431 whole cell lysates Lane 2: C6 whole cell lysates Lane 3: Hela whole cell lysates Lane 4: HUVEC whole cell lysates Lysates/proteins at 20 µg per lane. Secondary Goat Anti-mouse IgG, (H+L), Peroxidase conjugated at 1/10000 dilution Predicted band size : 36 kDa Blocking/Dilution buffer: 5% NFDM/TBST.

10320 Camino Santa Fe, Suite G
San Diego, CA 92121
Tel: 858.875.1900 Fax: 858.875.1999

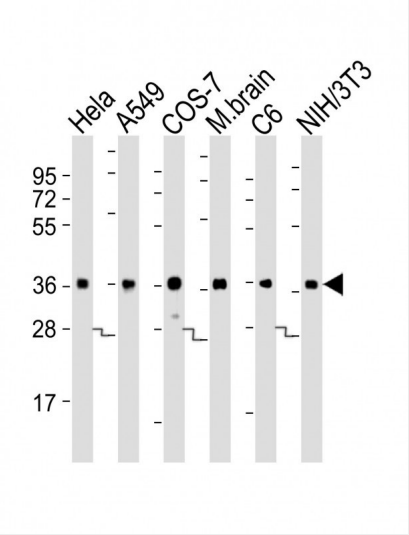

All lanes : Anti-GAPDH Antibody at 1:8000 dilution Lane 1: Hela whole cell lysates Lane 2: A549 whole cell lysates Lane 3: COS-7 whole cell lysates Lane 4: mouse brain lysates Lane 5: C6 whole cell lysates Lane 6: NIH/3T3 whole cell lysates Lysates/proteins at 20 µg per lane. Secondary Goat Anti-mouse IgG, (H+L), Peroxidase conjugated at 1/10000 dilution Predicted band size : 36 kDa Blocking/Dilution buffer: 5% NFDM/TBST.

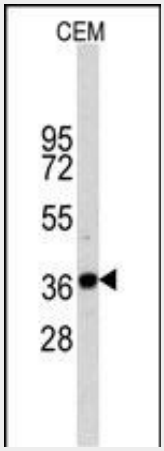

Western blot analysis of anti-GAPDH Monoclonal Antibody (Cat. #AM1020b) in CEM cell line lysates (35µg/lane). GAPDH(arrow) was detected using the purified Mab.

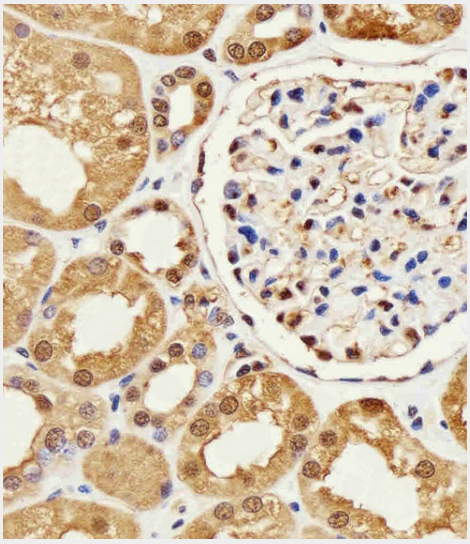

Immunohistochemical analysis of paraffin-embedded H.kidney section using GAPDH Antibody(Cat#AM1020b). AM1020b was diluted at 1:25 dilution. A peroxidase-conjugated goat anti-mouse IgG at 1:400 dilution was used as the secondary antibody, followed by DAB staining.

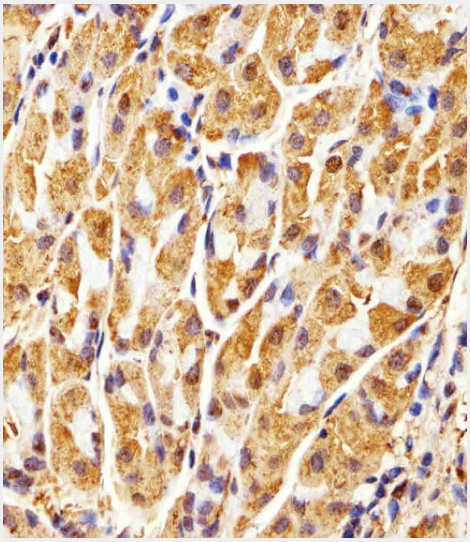

Immunohistochemical analysis of paraffin-embedded H.stomach section using GAPDH Antibody(Cat#AM1020b). AM1020b was diluted at 1:25 dilution. A peroxidase-conjugated goat anti-mouse IgG at 1:400 dilution was used as the secondary antibody, followed by DAB staining.

GAPDH Antibody - Background

The product of this gene catalyzes an important energy-yielding step in carbohydrate metabolism, the reversible oxidative phosphorylation of glyceraldehyde-3-phosphate in the presence of inorganic phosphate and nicotinamide adenine dinucleotide (NAD). The enzyme exists as a tetramer of identical chains. Many pseudogenes similar to this locus are present in the human genome.

GAPDH Antibody - References

Inhibition of glyceraldehyde-3-phosphate dehydrogenase activity by antibodies present in the cerebrospinal fluid of patients with multiple sclerosis. Kölln J, et al. J Immunol, 2010 Aug 1. PMID 20610654. Proteome analysis of the thalamus and cerebrospinal fluid reveals glycolysis dysfunction and potential biomarkers candidates for schizophrenia. Martins-de-Souza D, et al. J Psychiatr Res, 2010 May 14. PMID 20471030. Sex-specific proteome differences in the anterior cingulate cortex of schizophrenia. Martins-de-Souza D, et al. J Psychiatr Res, 2010 Apr 8. PMID 20381070. Identification of melanoma antigens using a Serological Proteome Approach (SERPA). Suzuki A, et al. Cancer Genomics Proteomics, 2010 Jan-Feb. PMID 20181627. siah-1 Protein is necessary for high glucose-induced glyceraldehyde-3-phosphate dehydrogenase nuclear accumulation and cell death in Muller cells. Yego EC, et al. J Biol Chem, 2010 Jan 29. PMID 19940145.

GAPDH Antibody - Citations

- CDK4/6 inhibitor palbociclib promotes SARS-CoV-2 cell entry by down-regulating SKP2 dependent ACE2 degradation
- Dl-3-n-butylphthalide alleviates cognitive impairment in amyloid precursor protein/presenilin 1 transgenic mice by regulating the striatal-enriched protein tyrosine phosphatase/ERK/cAMP-response element-binding protein signaling pathway
- Glutamate receptor, ionotropic, N-methyl D-aspartate-associated protein 1 promotes colorectal cancer cell proliferation and metastasis, and is negatively regulated by miR-296-3p
- DAB2IP decreases cell growth and migration and increases sensitivity to chemotherapeutic drugs in colorectal cancer

- RanBP2/Nup358 enhances miRNA activity by sumoylating Argonautes
- Down-Regulation of CIDEA Promoted Tumor Growth and Contributed to Cisplatin Resistance by Regulating the JNK-p21/Bad Signaling Pathways in Esophageal Squamous Cell Carcinoma
- Deoxycholic Acid Upregulates Serum Golgi Protein 73 through Activating NF-κB Pathway and Destroying Golgi Structure in Liver Disease
- A multi-kinase inhibitor APG-2449 enhances the antitumor effect of ibrutinib in esophageal squamous cell carcinoma via EGFR/FAK pathway inhibition
- Isochamaejasmin induces toxic effects on Helicoverpa zea via DNA damage and mitochondria-associated apoptosis
- CircRNA_102179 promotes the proliferation, migration and invasion in non-small cell lung cancer cells by regulating miR-330-5p/HMGB3 axis
- The E3 ubiquitin ligase UBR5 interacts with TTC7A and may be associated with very early onset inflammatory bowel disease
- Differential red blood cell age fractionation and Band 3 phosphorylation distinguish two different subtypes of warm autoimmune hemolytic anemia
- Ectodermal-neural cortex 1 as a novel biomarker predicts poor prognosis and induces metastasis in breast cancer by promoting Wnt/β-catenin pathway
- Circular RNA atlas in osteoclast differentiation with and without alendronate treatment
- miR-520h Stimulates Drug Resistance to Paclitaxel by Targeting the OTUD3-PTEN Axis in Breast Cancer
- Wall Teichoic Acid Glycosylation Promotes Surface Anchoring of Virulence Factors, Resistance to Antimicrobial Peptides, and Decreased Susceptibility to Antibiotics
- Iron overload contributes to general anaesthesia-induced neurotoxicity and cognitive deficits
- Long noncoding RNA atlas of the inflammation caused by asthma in mice
- Altered decidual and placental catabolism of vitamin D may contribute to the aetiology of spontaneous miscarriage
- Screening and identification of epithelial-to-mesenchymal transition-related circRNA and miRNA in prostate cancer
- Effect of Furostanol Saponins from Allium Macrostemon Bunge Bulbs on Platelet Aggregation Rate and PI3K/Akt Pathway in the Rat Model of Coronary Heart Disease.
- Induction of mTOR-dependent autophagy by WS nanosheets from both inside and outside of human cells.
- An in vitro model of foam cell formation induced by a stretchable microfluidic device.
- MicroRNA-26a inhibits multiple myeloma cell growth by suppressing cyclin-dependent kinase 6 expression.
- Exosomes increased angiogenesis in papillary thyroid cancer microenvironment.
- Inhibition of the deubiquitinase USP9x induces pre-B cell homeobox 1 (PBX1) degradation and thereby stimulates prostate cancer cell apoptosis.
- Downregulation of endothelial transient receptor potential vanilloid type 4 channel underlines impaired endothelial nitric oxide-mediated relaxation in the mesenteric arteries of hypertensive rats.
- Selenium-Rich Diet Induces Myocardial Structural and Functional Abnormalities by Activating Caspase-9 and Caspase-3 in Gpx-1P198L-Overexpression Transgenic Mice.
- Hepatitis C Virus Entry into Macrophages/Monocytes Mainly Depends on the Phagocytosis of Macrophages.
- The natural polyphenol curcumin induces apoptosis by suppressing STAT3 signaling in esophageal squamous cell carcinoma.
- l-Rhamnosylation of wall teichoic acids promotes efficient surface association of Listeria monocytogenes virulence factors InlB and Ami through interaction with GW domains.
- DFMG attenuates the activation of macrophages induced by co-culture with LPC-injured HUVE-12 cells via the TLR4/MyD88/NF-κB signaling pathway.
- Peptide SS-31 upregulates frataxin expression and improves the quality of mitochondria: implications in the treatment of Friedreich ataxia.
- Expression and prognostic significance of MYL9 in esophageal squamous cell carcinoma.

- The Role of Annexin A4 in Triple-Negative Breast Cancer Progression and Its Clinical Application.
- Use of rhenium-188 for in vivo imaging and treatment of human cervical cancer cells transfected with lentivirus expressing sodium iodide symporter.
- Silencing DNA methyltransferase 1 (DNMT1) inhibits proliferation, metastasis and invasion in ESCC by suppressing methylation of RASSF1A and DAPK.
- Pulsatile delivery of a leucine supplement during long-term continuous enteral feeding enhances lean growth in term neonatal pigs.
- Hepatocellular Carcinoma Cells Induce Regulatory T Cells and Lead to Poor Prognosis via Production of Transforming Growth Factor-β1.
- Upregulation of microRNA-96 and its oncogenic functions by targeting CDKN1A in bladder cancer.
- SC06, a novel small molecule compound, displays preclinical activity against multiple myeloma by disrupting the mTOR signaling pathway.
- Molecular In Vivo Imaging Using a Noninvasive Cardiac-Specific MLC-2v Promoter Driven Dual-Gene Recombinant Lentivirus Monitoring System.
- Cyclin O regulates germinal vesicle breakdown in mouse oocytes.
- Nutrition deficiency promotes apoptosis of cartilage endplate stem cells in a caspase-independent manner partially through upregulating BNIP3.